

Supplementary Information

Dysprosium Complexes Bearing Unsupported Dy^{III}–Ge^{II}/Sn^{II} Metal–Metal Bonds as Single-Ion Magnets

Shi-Ming Chen, Jin Xiong, Yi-Quan Zhang, Fang Ma, Hao-Ling Sun, Bing-Wu Wang*,
Song Gao*

Abstract: Two dysprosium complexes bearing unsupported Dy–Ge/Sn metal–metal bonds are reported here with their syntheses, single crystal structures, bonding character and magnetic properties. Natural bond orbital (NBO) analysis revealed that Dy–Ge and Dy–Sn bonds both contain relatively large covalency. Measurements of magnetic dynamics uncovered that they exhibit slow relaxation of magnetization under a zero applied direct current (DC) field with energy barriers of 485 and 620 K respectively and the blocking temperatures of 6 K. Through bonding with electropositive metal ions, Dy^{III} centers retain strong uniaxial magnetic anisotropy.

Table of Contents

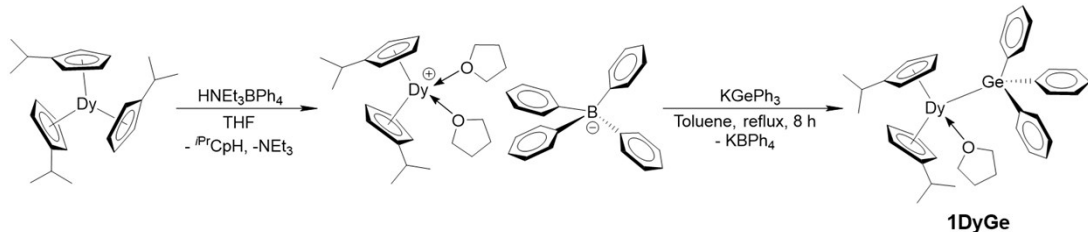
1. Experimental Procedures.....	3
1.1. General considerations.....	3
1.2. Synthesis of [(<i>i</i> PrCp) ₂ DyGePh ₃ (THF)] (1DyGe)	3
1.3. Synthesis of [(Cp [*]) ₂ DySnPh ₃ (THF)] (1DySn).....	4
2. Crystallographic Data	4
2.1. Data collection and refinement	4
2.2. Single crystal structures of 1DyGe and 1DySn	5
3. Magnetic Properties.....	7
3.1. Static magnetic properties of 1DyGe	7
3.2. Magnetic hysteresis of 1DyGe	7
3.3. Magnetic dynamics of 1DyGe	9
3.4. Static magnetic properties of 1DySn	12
3.5. Magnetic hysteresis of 1DySn	12
3.6 Magnetic dynamics of 1DySn	14
4. Computation.....	17
4.1 <i>Ab initio</i> calculation for 1DyGe	17
4.2 <i>Ab initio</i> calculation for 1DySn	20
4.3. Bonding Analyses	22
References.....	31

1. Experimental Procedures

1.1. General considerations

All reactions and manipulations described below were carried out under anhydrous and anaerobic conditions using standard Schlenk line techniques and Ar-filled glove box. Tetrahydrofuran (THF), toluene and hexanes were degassed and dehydrated by MBraun solvent purification system. Superdry DyCl₃, Cp*H, KN(SiMe₃)₂, (*i*PrCp)₃Dy, HGePh₃, HSnPh₃, ClMg(C₃H₅) (1.7 M in THF), anhydrous 1,4-dioxane are commercially available. HNEt₃BPh₄^[1], KGePh₃^[2], KCp*^[3], (Cp*)₂DyCl₂K^[3], (Cp*)₂Dy(C₃H₅)^[3], (Cp*)₂DyBPh₄^[3] were prepared according to previous literatures. Elemental analyses were performed on the Vario EL CUBE Elemental Analyzer.

1.2. Synthesis of [(*i*PrCp)₂DyGePh₃(THF)] (1DyGe)



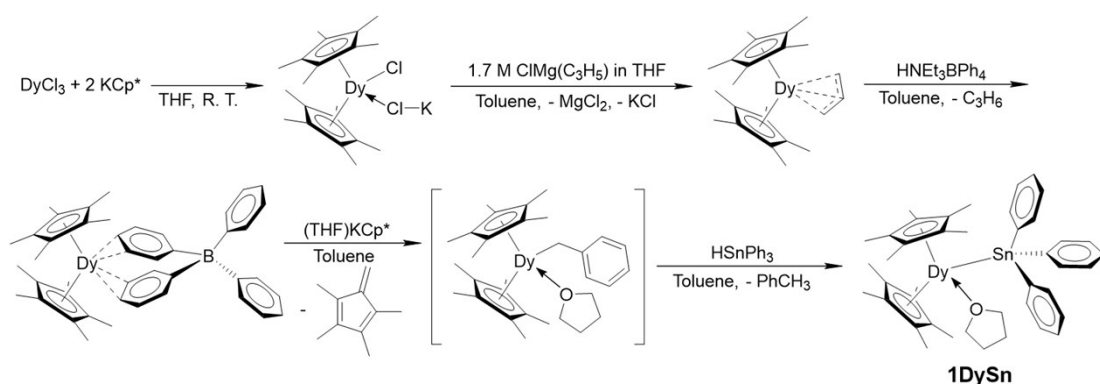
Scheme S1. Synthesis of 1DyGe.

2.4202 g (5 mmol) of (*i*PrCp)₃Dy was dissolved in THF. 2.1072 g (5 mmol) of HNEt₃BPh₄ was suspended in THF and then added slowly to above solution dropwise at room temperature. A large amount of white microcrystals precipitate almost immediately. The reaction lasted overnight. Then the solvent was removed under vacuum. White microcrystals were obtained and then washed using as little THF as possible. Extra white product could be isolated by concentration of THF washings. Collect the white microcrystals and then recrystallize in THF. After several days, light yellow crystals of (*i*PrCp)₂Dy(THF)₂BPh₄ were obtained, and then washed by a little bit of THF followed by drying. Yield: 2.8916 g, 68.8%. Analytically calculated for (*i*PrCp)₂Dy(THF)₂BPh₄: C, 68.61%; H, 6.96%; found: C, 68.83%; H, 7.07%.

0.8403 g (1 mmol) of (*i*PrCp)₂Dy(THF)₂BPh₄ and 0.3431 g (1 mmol) of KGePh₃ were suspended in 15 mL of toluene and then heated to 80 °C. The reaction lasted overnight. After cooled to room temperature, the reaction solution was filtered to remove KBPh₄, and then the filtrate was concentrated. Light yellow single crystals of (*i*PrCp)₂DyGePh₃(THF) (**1DyGe**) suitable for X-ray diffraction analysis were obtained by cooling the concentrated solution at -30 °C for several weeks. Yield: 0.4644 g, 61.7%. Analytically calculated for **1DyGe**: C, 60.62%; H, 6.02%; found: C, 61.06%; H, 6.07%.

1.3. Synthesis of $[(\text{Cp}^*)_2\text{DySnPh}_3(\text{THF})]$ (**1DySn**)

0.8745 g (1.16 mmol) of $(\text{Cp}^*)_2\text{DyBPh}_4$ was suspended in 10 mL of toluene. The suspension of 0.2027 g (1.16 mmol) of KCp^* in toluene was slowly added dropwise to the above solution at room temperature, and the reaction mixture turned light orange about two minutes later. It signifies the production of $(\text{Cp}^*)_2\text{DyCH}_2\text{Ph}$ ^[4]. After about 5 h, a toluene solution of 0.4072 g (1.16 mmol) of HSnPh_3 was added slowly to the above mixture at ambient temperature. The color of reaction mixture turned from light orange to yellow in several minutes. The reaction lasted overnight followed by filtration. The filtrate was concentrated under vacuum. Cooling the concentrated solution at -30°C for several days afforded orange-yellow single crystals suitable for X-ray diffraction. Yield: 0.4322 g, 43.6%. Analytically calculated for **1DySn**: C, 58.99%; H, 6.25%; found: C, 59.65%; H, 6.34%.



Scheme S2. Synthesis of **1DySn**.

2. Crystallographic Data

2.1. Data collection and refinement

The crystals were wrapped in mineral oil and then were frozen in 180 K. Data collections were performed at 180 K on a SuperNova diffractometer using graphite-monochromated Mo $\text{K}\alpha$ radiation ($\lambda = 0.71073 \text{ \AA}$). Using Olex2^[5], the structure was solved with the Superflip structure solution program using Charge Flipping^[6] and refined with the ShelXL refinement package using Least Squares minimization. Refinement was performed on F^2 anisotropically for all of the nonhydrogen atoms by the full-matrix least-squares method. The hydrogen atoms were placed at the calculated positions and were included in the structure calculation without further refinement of their parameters. Crystallographic data (excluding structure factors) have been deposited with the Cambridge Crystallographic Data Centre with supplementary publication numbers: 1864988 for **1DyGe** and 1864989 for **1DySn**. These data can be obtained free of charge from the Cambridge Crystallographic Data Centre via <https://www.ccdc.cam.ac.uk/structures/>.

2.2. Single crystal structures of **1DyGe** and **1DySn**

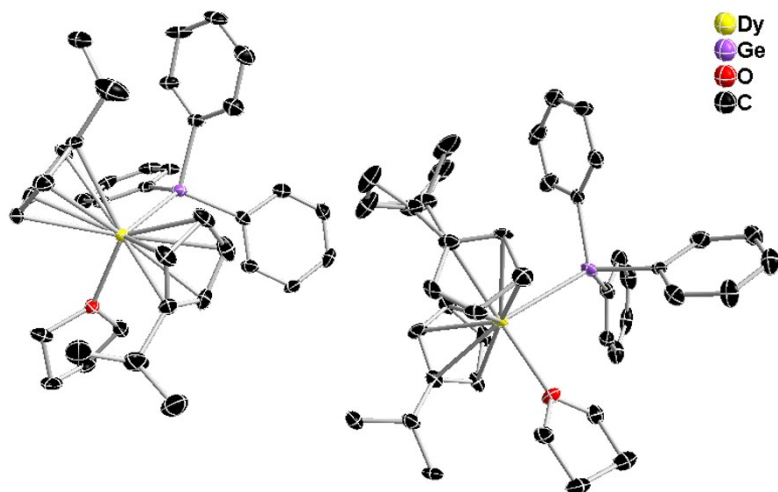


Figure S1. Molecular structure of two inequivalent **1DyGe** as an asymmetric unit in lattice. Yellow, purple, red and black ellipsoids (30% probability) represent Dy, Ge, O and C, respectively. Hydrogen atoms have been omitted for clarity.

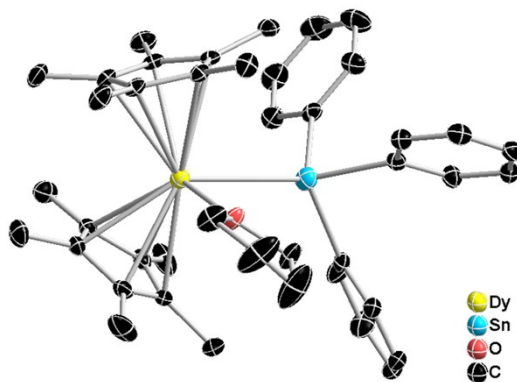


Figure S2. Molecular structure of **1DySn**. Yellow, blue, red and black ellipsoids (30% probability) represent Dy, Sn, O and C, respectively. Hydrogen atoms have been omitted for clarity.

Table S1. Crystallographic data of **1DyGe** and **1DySn**

Formula	C₃₈H₄₅ODyGe (1DyGe)	C₄₂H₅₃ODySn (1DySn)
Formula Weight	752.91	855.10
T, K	180	180
λ , Å	0.710	0.710
Crystal System	Monoclinic	Monoclinic
Space Group	P2 ₁ /c	P2 ₁ /c
a, Å	14.1320(5)	12.6271(4)
b, Å	20.8389(7)	17.0698(2)
c, Å	22.9987(9)	23.3096(8)
β , degree	94.211(3)	132.134(6)
Z	8	4
V, Å ³	6754.7(4)	3725.8(3)
D _c , g cm ⁻³	1.481	1.524
F(000)	3032.0	1716.0
μ , mm ⁻¹	3.112	2.690
R ₁ (reflections)	0.0689	0.0199
wR ₂ (reflections)	0.1789	0.0487
S	1.057	1.040

Table S2. Selected bond lengths of **1DyGe** and **1DySn**

Bonds/Å	C₃₈H₄₅ODyGe (1DyGe)	C₄₂H₅₃ODySn (1DySn)
Dy–E (E = Ge, Sn)	2.973(1)/2.988(1)	3.239(0)
Dy–C1	2.659(10)/2.670(10)	2.710(2)
Dy–C2	2.665(10)/2.677(10)	2.682(2)
Dy–C3	2.670(11)/2.684(10)	2.653(2)
Dy–C4	2.610(10)/2.623(9)	2.692(3)
Dy–C5	2.601(11)/2.582(12)	2.687(3)
Dy–C6	2.653(9)/2.651(9)	2.682(3)
Dy–C7	2.656(10)/2.662(9)	2.703(2)
Dy–C8	2.637(9)/2.634(10)	2.683(3)
Dy–C9	2.635(9)/2.630(9)	2.660(3)
Dy–C10	2.649(10)/2.639(9)	2.649(4)
Dy–Cp _c 1	2.355/2.358	2.398(0)
Dy–Cp _c 2	2.358/2.369	2.390(0)
Dy–O	2.3524(5)/2.361(6)	2.370(2)
Shortest Dy···Dy	8.769(1)	9.627(1)

* C_p_c is the centroid of five-membered aromatic ring.

Table S3. Selected angles of **1DyGe** and **1DySn**

Angles /°	$C_{38}H_{45}ODyGe$ (1DyGe)	$C_{42}H_{53}ODySn$ (1DySn)
O–Dy–E (E = Ge, Sn)	96.7(2)/93.3(1)	91.5
Cp_c –Dy– Cp_c	132.6(4)/129.1(4)	134.8(1)

3. Magnetic Properties

Samples were closely wrapped by two layers of para-films followed by plugged into a capsule in glovebox, and then fixed in a straw. This straw was placed in a Schlenk tube before being transferred out of glovebox. Direct current (DC) susceptibilities and alternative current (AC) magnetic susceptibilities with frequencies ranging from 1 to 997 Hz were performed on a Quantum Design MPMS2 XL-5 SQUID magnetometer on polycrystalline samples. AC susceptibility measurement with frequencies ranging from 100 to 10000 Hz was performed on a Quantum Design PPMS on polycrystalline samples. Magnetic hysteresis measurements were carried out on a Quantum Design MPMS3 SQUID magnetometer. All DC magnetic susceptibilities were corrected for diamagnetic contribution from the sample holder, para-films, capsules and diamagnetic contributions from the molecule using Pascal's constants^[7].

3.1. Static magnetic properties of **1DyGe**

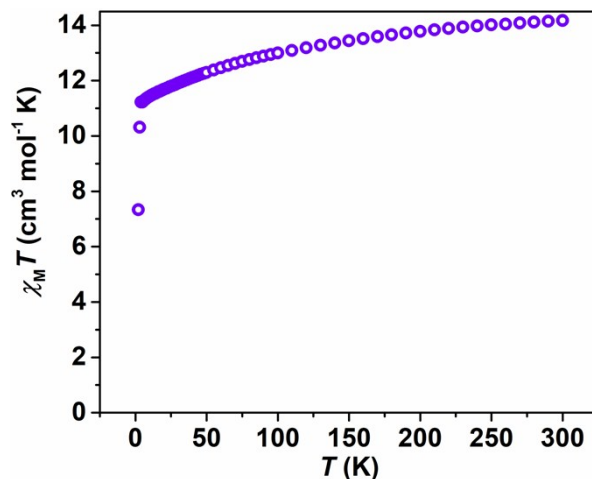


Figure S3. Temperature dependence of the static molar magnetic susceptibility times temperature ($\chi_M T$) for **1DyGe** under an applied static field of 1000 Oe over the temperature range from 2 to 300 K.

3.2. Magnetic hysteresis of **1DyGe**

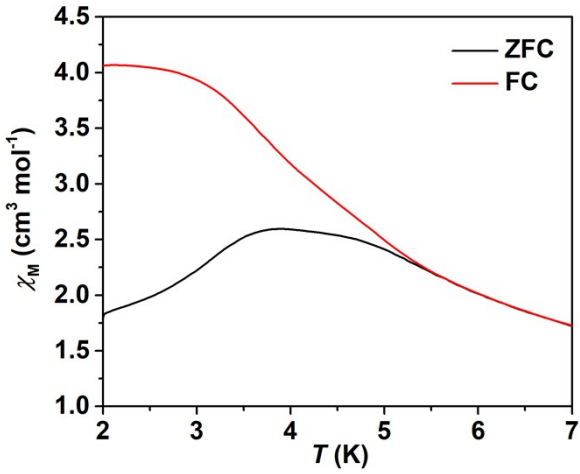


Figure S4. Plot of zero-field cooled (ZFC, black line) and field-cooled (FC, red line, $H_{DC} = 1000$ Oe) magnetic susceptibility of **1DyGe** versus temperature.

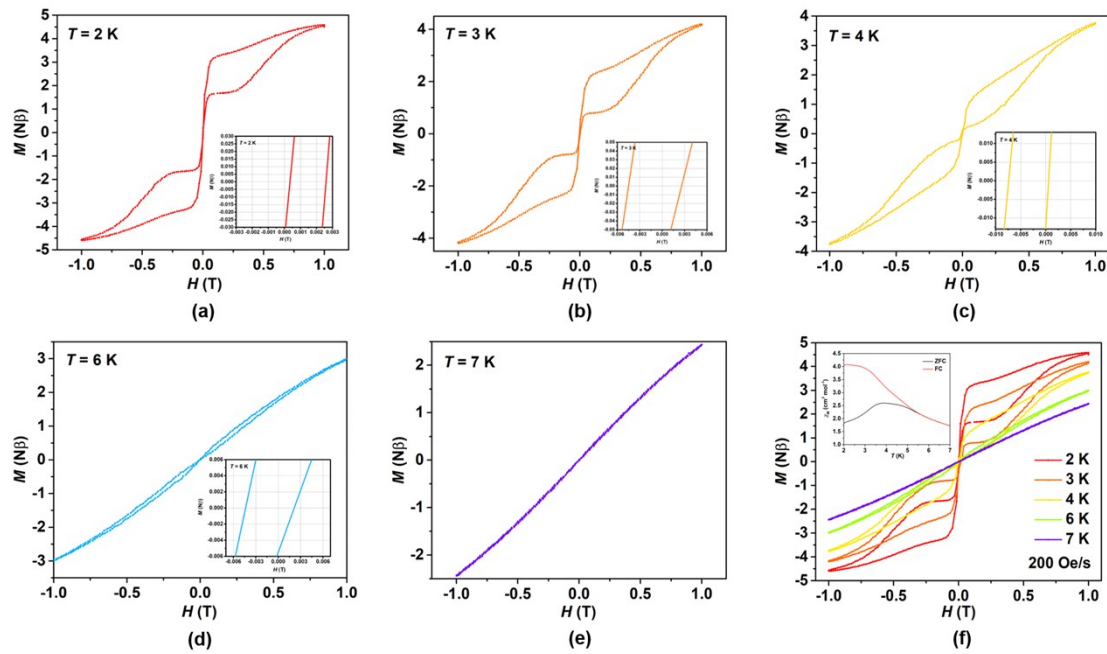


Figure S5. Magnetic hysteresis loops for **1DyGe** with a field-sweeping rate of 200 Oe/s at 2, 3, 4, 6, 7 K, respectively.

3.3. Magnetic dynamics of 1DyGe

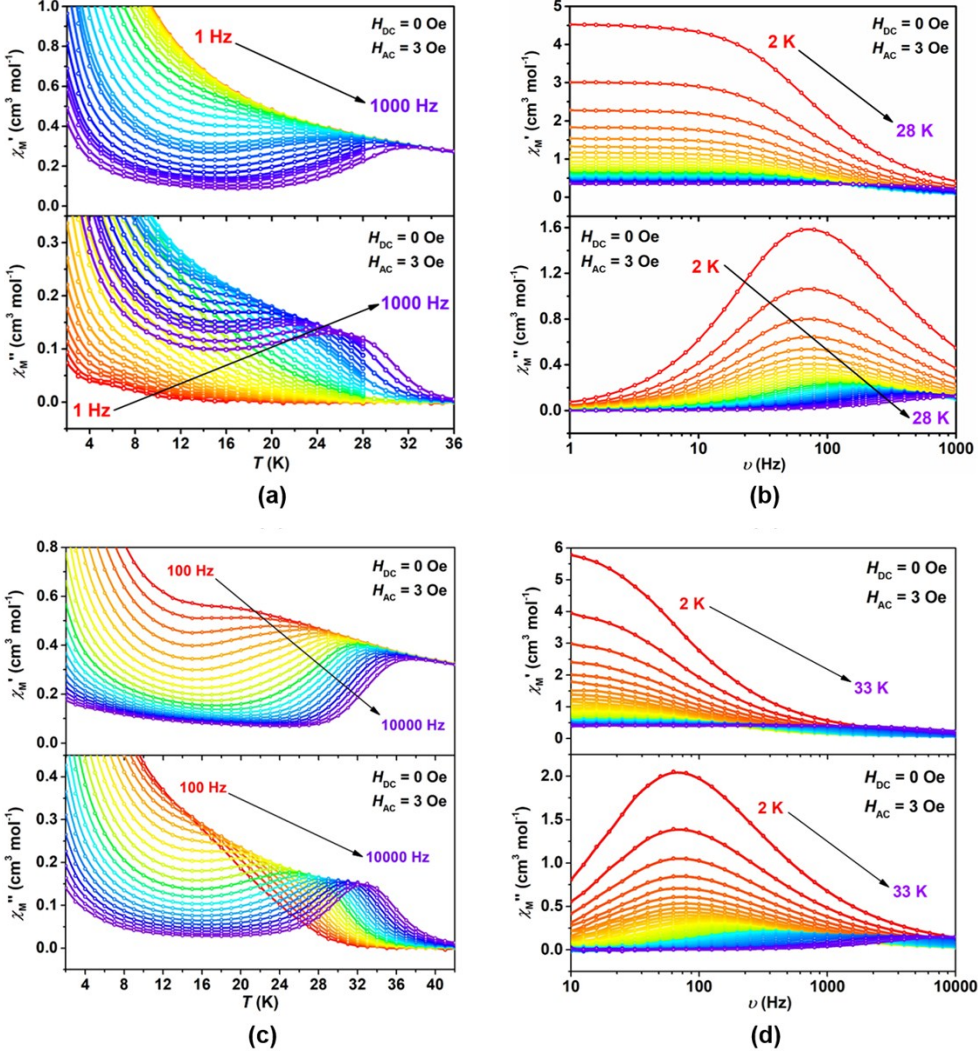


Figure S6. Temperature- (a, c) and frequency-dependence (b, d) of in-phase (χ_M' , upper) and out-of-phase (χ_M'' , lower) molar AC susceptibility for **1DyGe** under a zero applied DC magnetic field. **a, b:** data derived from MPMS, and **c, d:** data derived from PPMS.

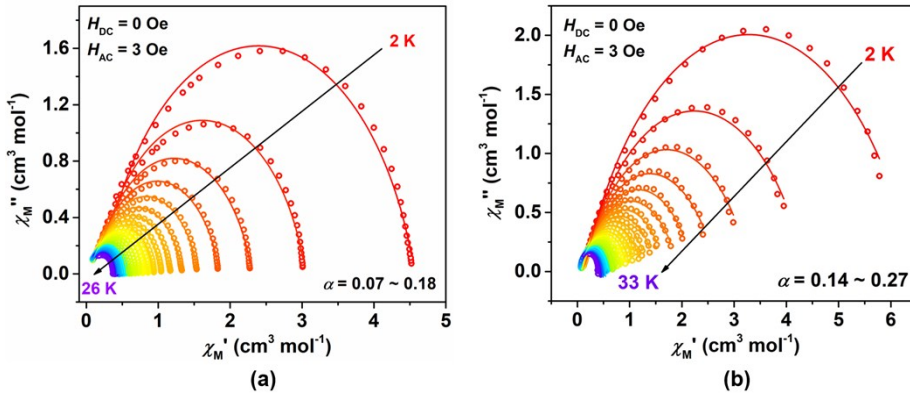


Figure S7. Argand plots of χ_M'' vs χ_M' for **1DyGe** under a zero applied DC magnetic field (**a:** data derived from MPMS, **b:** data derived from MPMS).

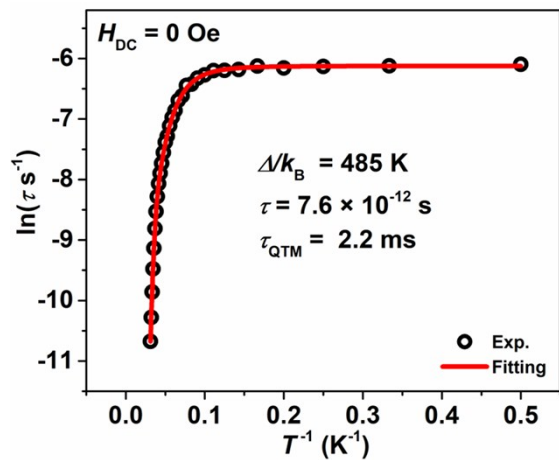


Figure S8. Plot of natural log of relaxation time *versus* inverse temperature. The red solid line represents the best fitting using a combination of Orbach, Raman and QTM process. The fitting gives relaxation barrier $\Delta/k_B = 485 \text{ K}$ and $\tau_0 = 7.6 \times 10^{-12} \text{ s}$.

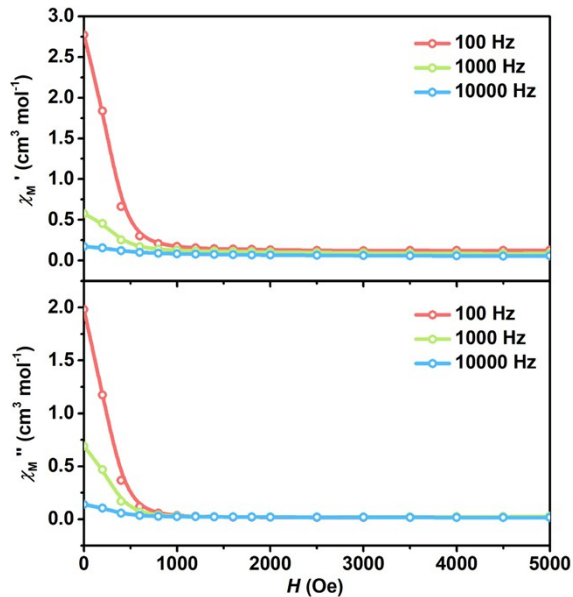


Figure S9. Plot of in-phase (χ_M' , upper) and out-of-phase (χ_M'' , lower) molar AC susceptibility for **1DyGe** *vs* applied DC fields under AC magnetic field with oscillation frequency of 100, 1000, 10000 Hz, respectively.

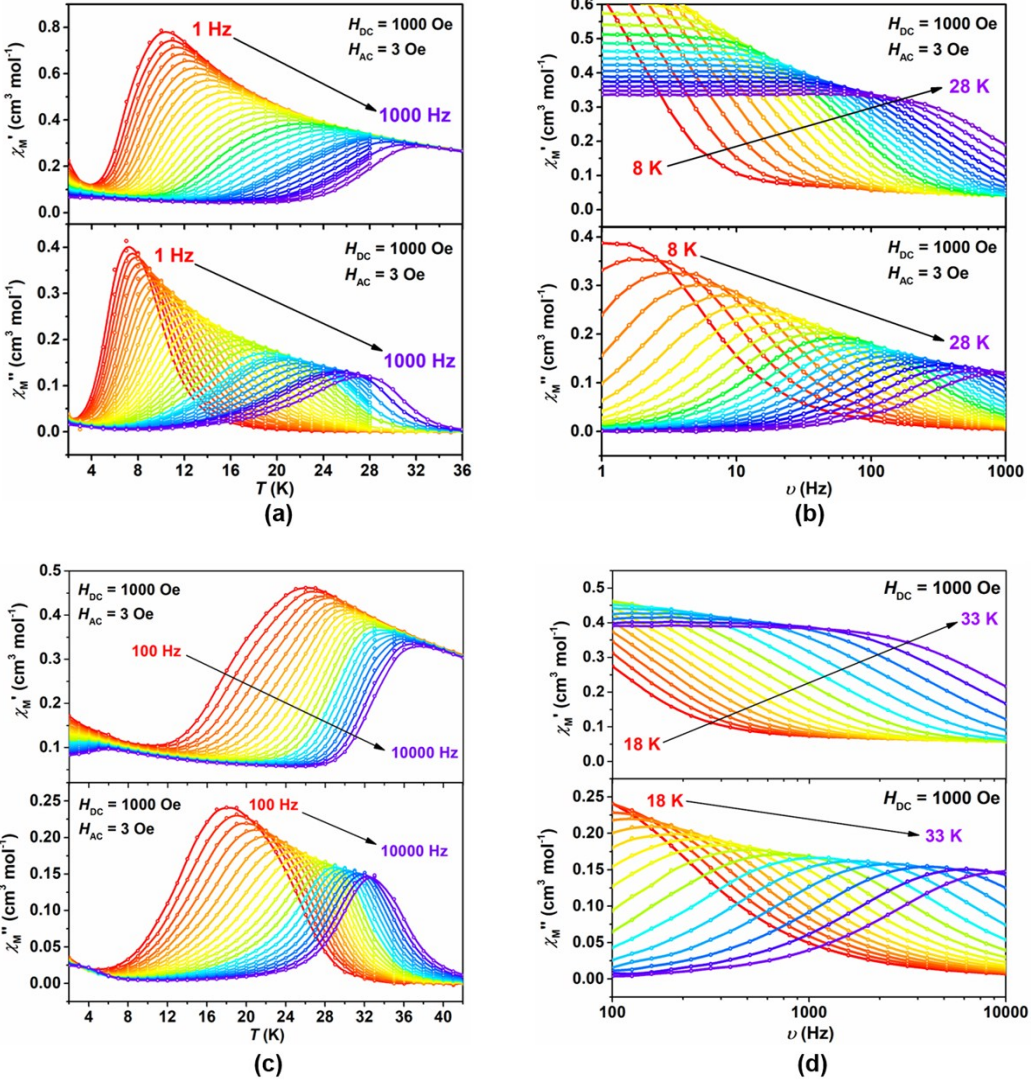


Figure S10. Temperature- (**a, c**) and frequency-dependence (**b, d**) of in-phase (χ_M' , upper) and out-of-phase (χ_M'' , lower) molar AC susceptibility for **1DyGe** under a 1000 Oe of DC magnetic field. **a, b**: data derived from MPMS, and **c, d**: are data derived from PPMS.

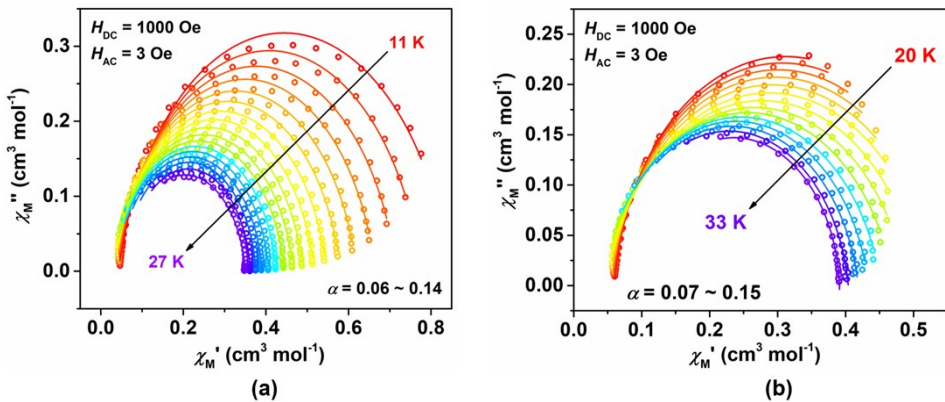


Figure S11. Argand plots of χ_M'' vs χ_M' for **1DyGe** under a 1000 Oe of DC magnetic field (**a**: data derived from MPMS, **b**: data derived from PPMS).

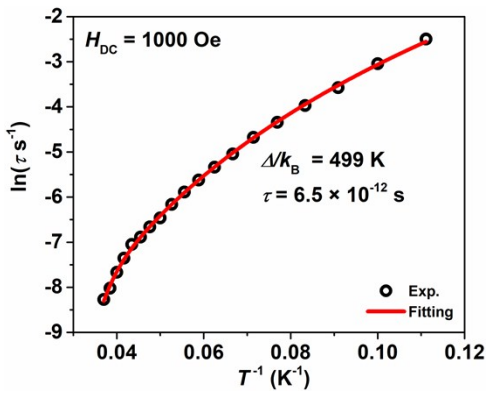


Figure S12. Plot of natural log of relaxation time *versus* inverse temperature. The red solid line represents the best fitting using a combination of Orbach and Raman process. The fitting gives relaxation barrier $\Delta/k_{\text{B}} = 499 \text{ K}$ and $\tau_0 = 6.5 \times 10^{-12} \text{ s}$.

3.4. Static magnetic properties of **1DySn**

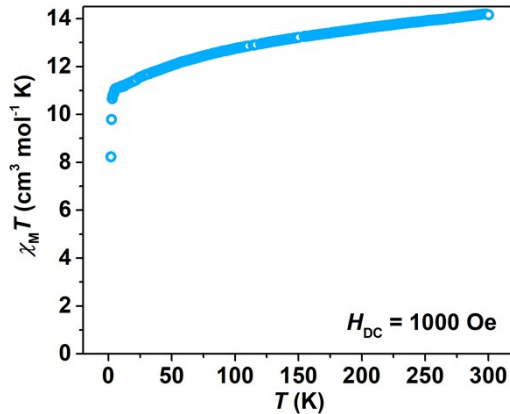


Figure S13. Temperature dependence of the static molar magnetic susceptibility times temperature ($\chi_M T$) for **1DySn** under an applied static field of 1000 Oe over the temperature range from 2 to 300 K.

3.5. Magnetic hysteresis of **1DySn**

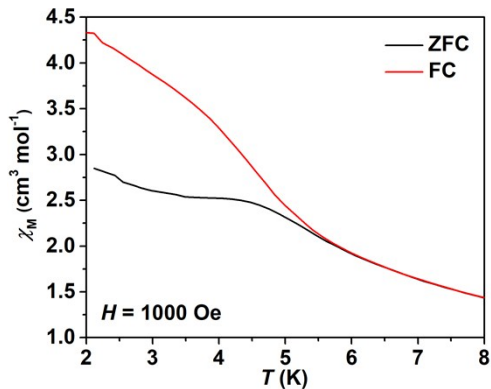


Figure S14. Plot of zero-field cooled (ZFC, black line) and field-cooled (FC, red line, $H_{\text{DC}} = 1000 \text{ Oe}$) magnetic susceptibility of **1DySn** *versus* temperature.

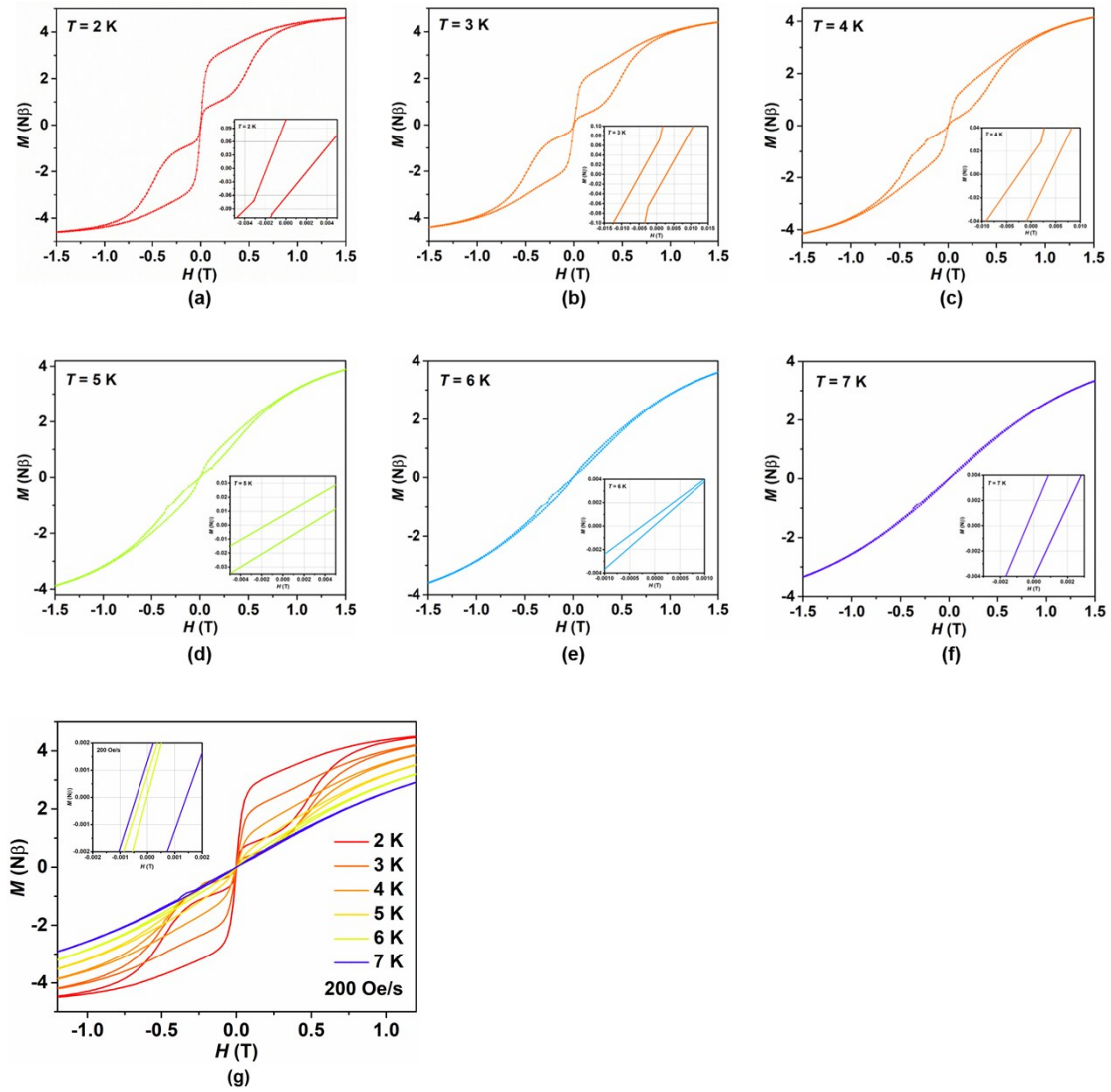


Figure S15. Magnetic hysteresis loops for **1DySn** with a field-sweeping rate of 200 Oe/s at 2, 3, 4, 5, 6, 7 K, respectively.

3.6 Magnetic dynamics of 1DySn

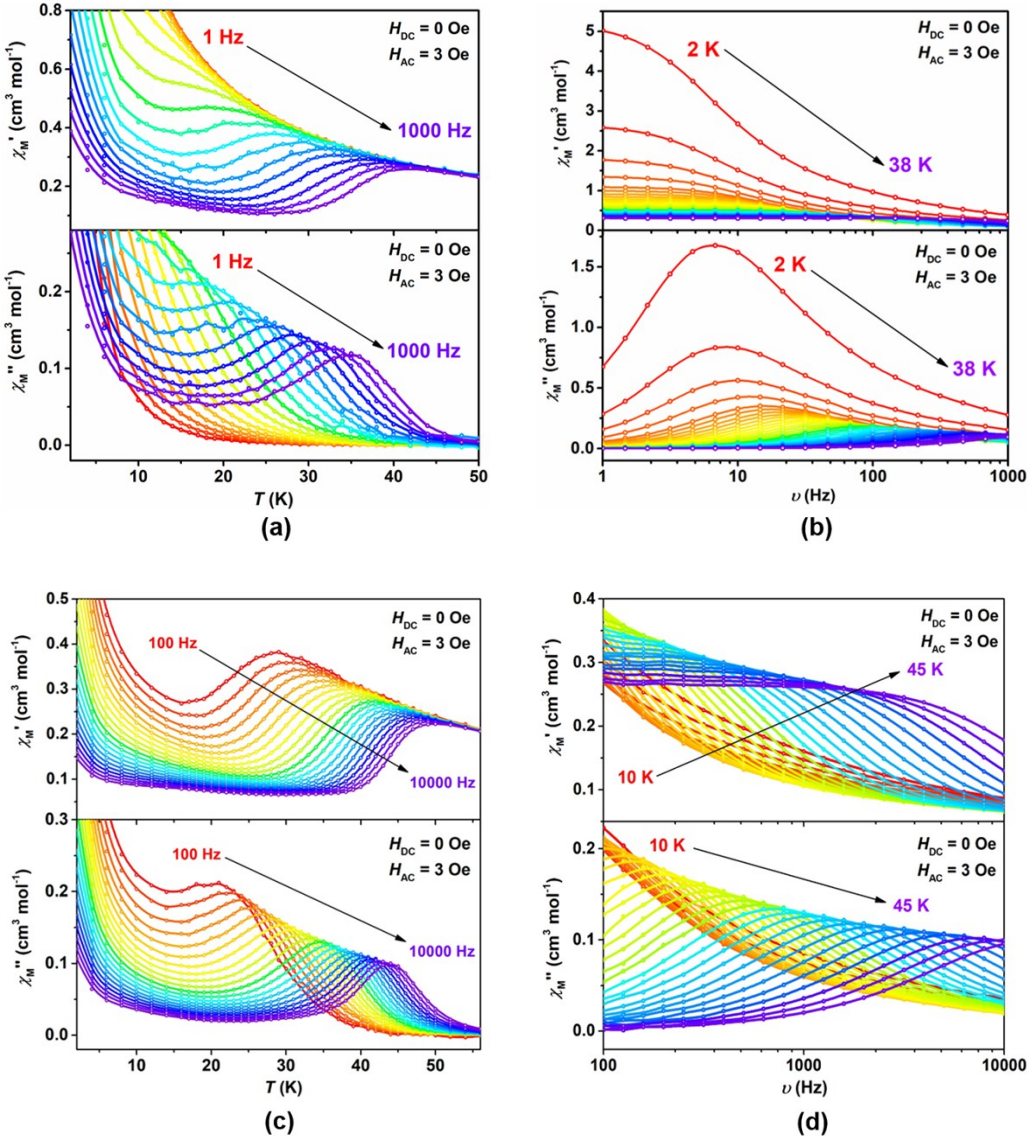


Figure S16. Temperature- (a, c) and frequency-dependence (b, d) of in-phase (χ_M' , upper) and out-of-phase (χ_M'' , lower) molar AC susceptibility for **1DySn** under a zero applied DC magnetic field. **a, b:** data derived from MPMS, and **c, d:** data derived from PPMS.

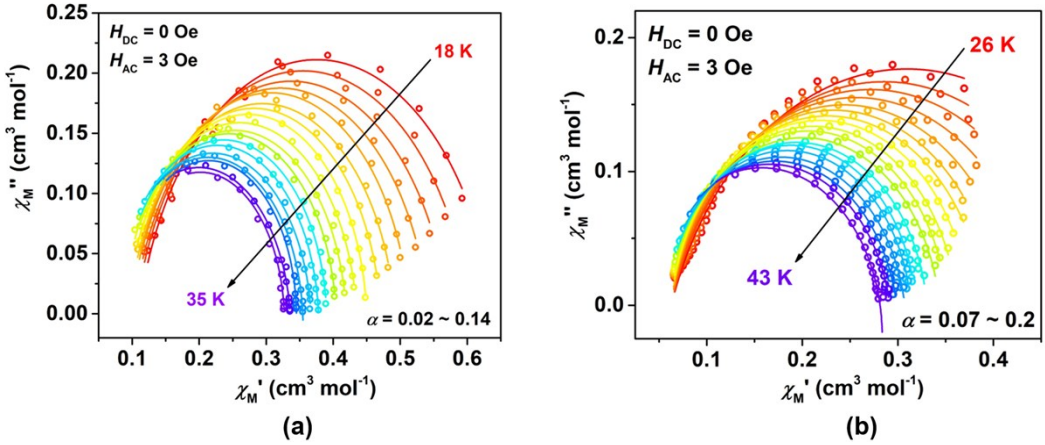


Figure S17. Argand plots of χ_M'' vs χ_M' for **1DySn** under a zero applied DC magnetic field (**a**: data derived from MPMS, **b**: data derived from MPMS).

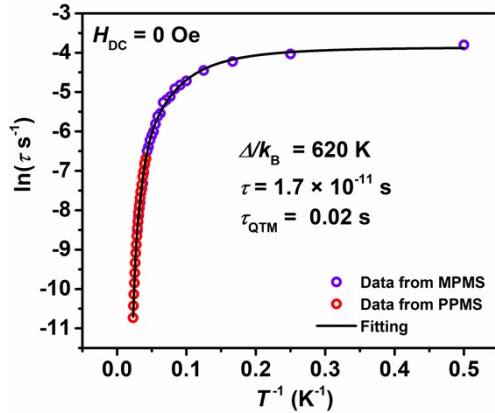


Figure S18. Plot of natural log of relaxation time *versus* inverse temperature. The red and purple circles represent the data from PPMS and MPMS, respectively. The black solid line represents the best fitting using a combination of Orbach and QTM process. The fitting gives energy barrier $\Delta/k_B = 620$ K and $\tau_0 = 1.7 \times 10^{-11}$ s.

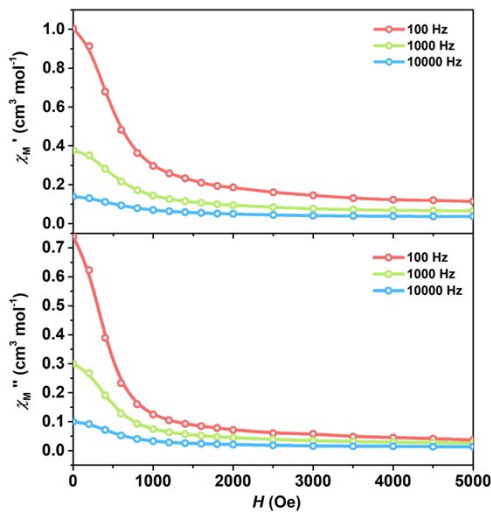


Figure S19. Plot of in-phase (χ_M' , upper) and out-of-phase (χ_M'' , lower) molar AC susceptibility for **1DySn** *vs* field under AC magnetic field with oscillation frequency of 100, 1000, 10000 Hz, respectively.

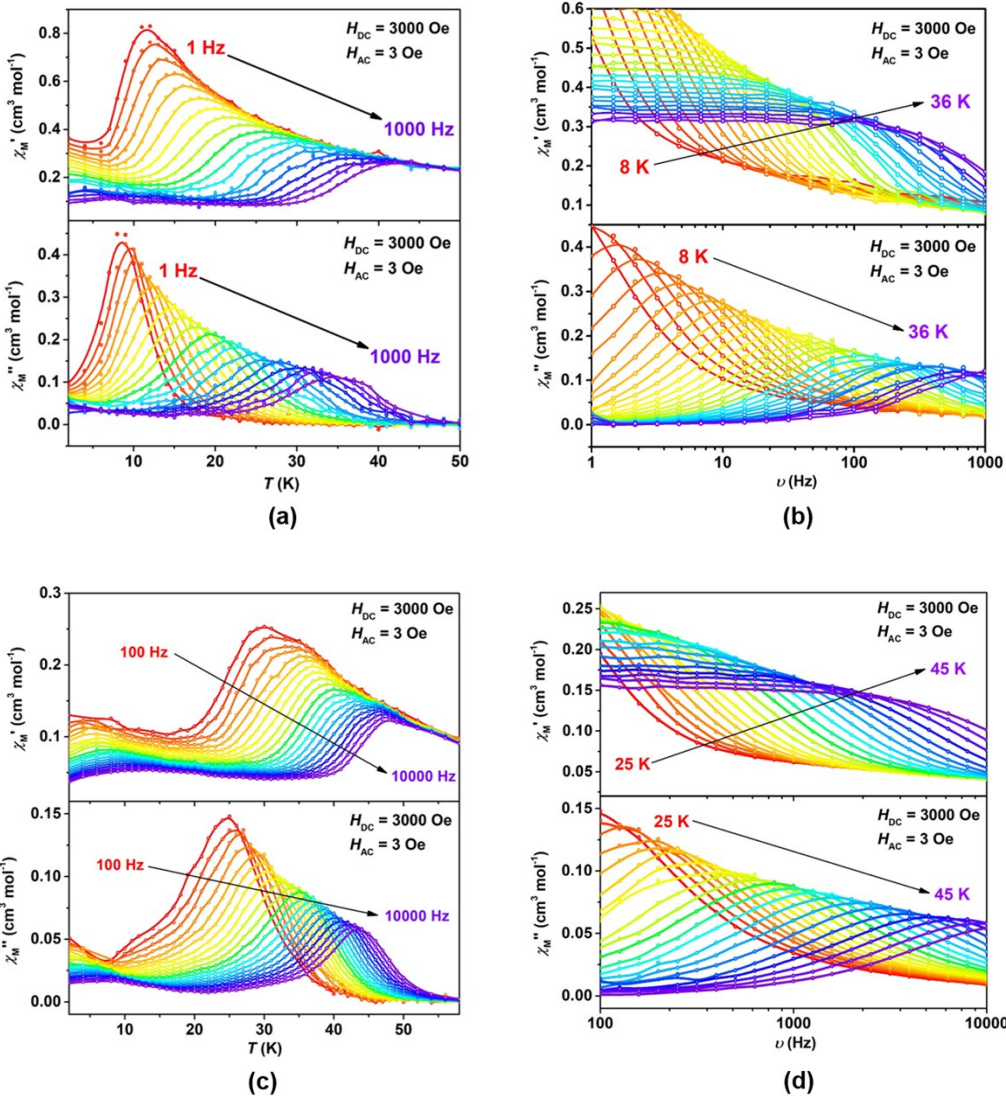


Figure S20. Temperature- **(a, c)** and frequency-dependence **(b, d)** of in-phase (χ_M' , upper) and out-of-phase (χ_M'' , lower) molar AC susceptibility for **1DySn** under a 3000 Oe of DC magnetic field. **a, b:** are data derived from MPMS, and **c, d:** are data derived from PPMS.

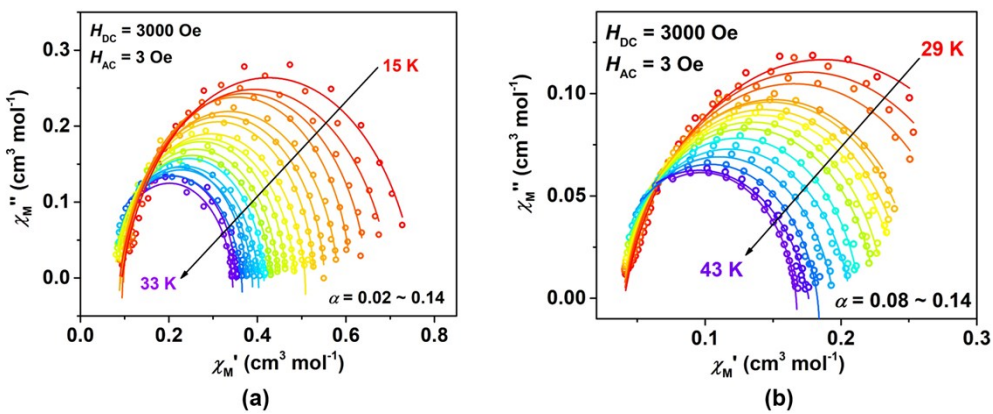


Figure S21. Argand plots of χ_M'' vs χ_M' for **1DySn** under a 3000 Oe of DC magnetic field **(a:** data derived from MPMS, **b:** data derived from MPMS).

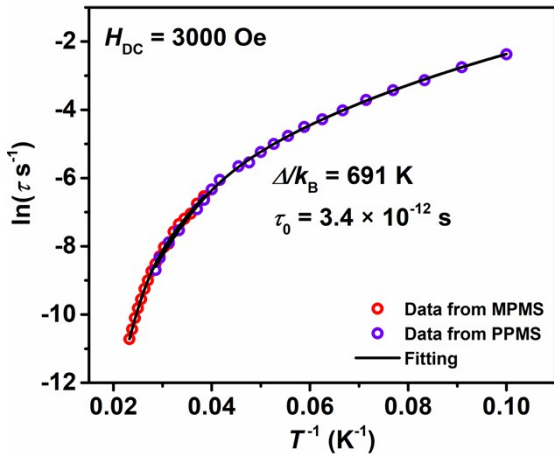


Figure S22. Plot of natural log of relaxation time *versus* inverse temperature. The red and purple circles represent the data from PPMS and MPMS, respectively. The black solid line represents the best fitting using a combination of Orbach and QTM process. The fitting gives energy barrier $\Delta/k_B = 691 \text{ K}$ and $\tau_0 = 3.4 \times 10^{-12} \text{ s}$.

4. Computation

4.1 *Ab initio* calculation for 1DyGe

Mononuclear complex **1DyGe** has two different molecular structures indicated as Dy1 and Dy2 (see Fig. S23). Complete-active-space self-consistent field (CASSCF) calculations on Dy1 and Dy2 of 1DyGe extracted from the compound on the basis of single crystal X-ray determined geometry have been carried out with MOLCAS 8.2^[8] program package.

The basis sets for all atoms are atomic natural orbitals from the MOLCAS ANO-RCC library: ANO-RCC-VTZP for Dy^{III}; VTZ for close C and O; VDZ for distant atoms. The calculations employed the second order Douglas-Kroll-Hess Hamiltonian, where scalar relativistic contractions were taken into account in the basis set and the spin-orbit couplings were handled separately in the restricted active space state interaction (RASSI-SO) procedure. Active electrons in 7 active spaces include all *f* electrons (CAS (9 in 7) for Dy1 and Dy2) in the CASSCF calculation. To exclude all the doubts, we calculated all the roots in the active space. We have mixed the maximum number of spin-free state which was possible with our hardware (all from 21 sextets, 128 from 224 quadruplets, 130 from 490 doublets for Dy^{III}). Single-Aniso^[9] program was used to obtain the energy levels, *g* tensors, *m_j* values, magnetic axes, *et al.*, based on the above CASSCF/RASSI calculations.

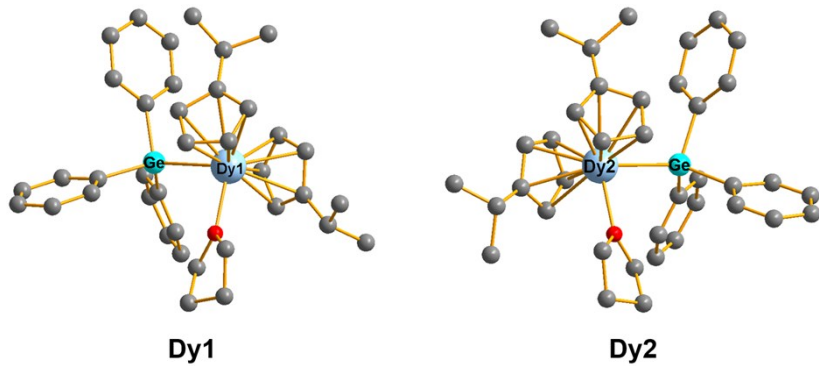


Figure S23. Calculated structures of Dy1 and Dy2 of **1DyGe**; H atoms are omitted.

Table S4. Calculated energy levels (cm^{-1}), g (g_x, g_y, g_z) tensors and m_J values of the lowest eight Kramers doublets (KDs) of Dy1 and Dy2 for **1DyGe**.

KDs	Dy1			Dy2		
	E/cm^{-1}	g	m_J	E/cm^{-1}	g	m_J
1	0.0 19.407	0.005 0.007	$\pm 15/2$	1	0.0 19.308	0.009 $\pm 15/2$
2	136.4 16.776	0.087 0.113	$\pm 13/2$	2	134.0 16.733	0.119 0.154
3	256.5 11.400	2.497 5.744	$\pm 11/2$	3	260.7 2.959	10.146 8.002
4	289.1 0.930	8.330 5.915	$\pm 5/2$	4	292.9 7.793	3.388 3.716
5	327.0 13.040	1.358 3.582	$\pm 9/2$	5	343.8 11.166	2.759 4.876
6	359.3 13.759	0.039 2.450	$\pm 3/2$	6	384.6 14.498	0.699 1.825
7	396.1 16.075	0.955 2.103	$\pm 7/2$	7	431.0 16.707	0.653 1.117
8	516.3 19.732	0.063 0.125	$\pm 1/2$	8	571.3 19.739	0.051 0.087

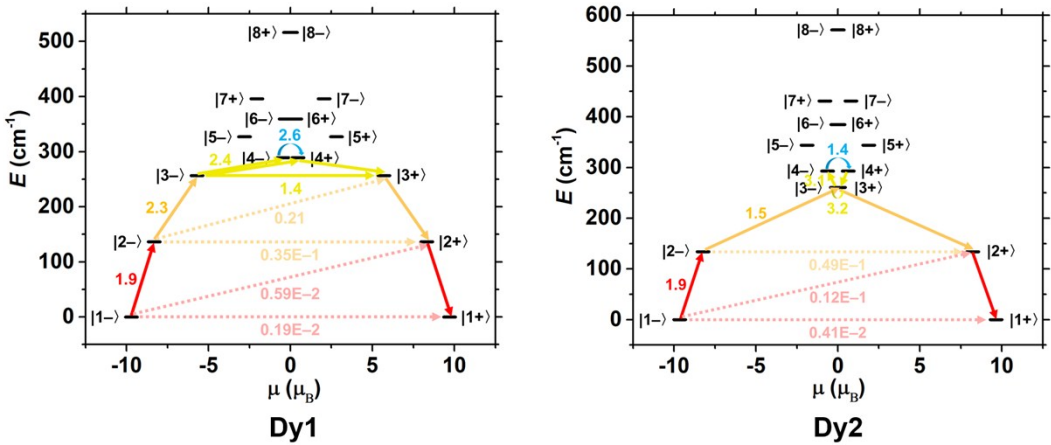


Figure S24. Magnetization blocking barriers for Dy1 and Dy2 for **1DyGe**. The thick black lines represent the Kramers doublets as a function of their magnetic moment along the magnetic axis. The solid arrows represent the most probable path for magnetic relaxation in the corresponding compounds. The numbers at each arrow stand for the mean absolute value of the corresponding matrix element of transition magnetic moment.

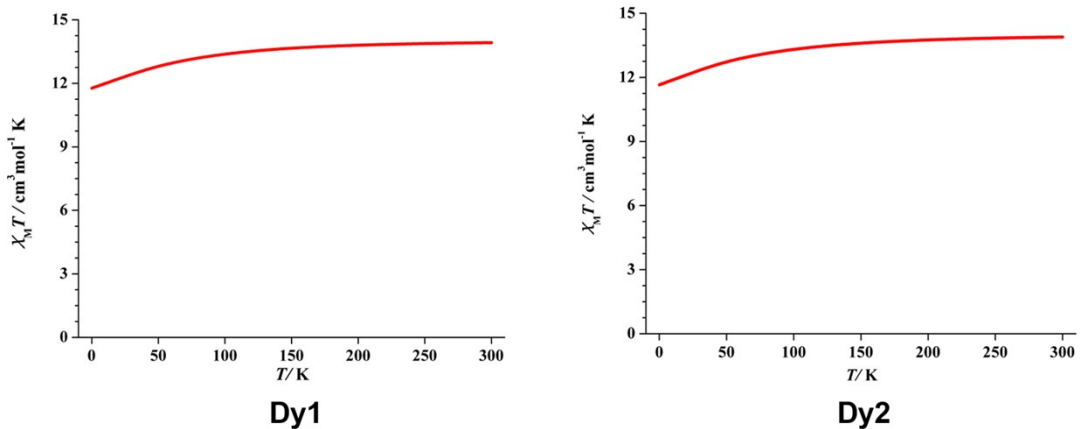


Figure S25. Calculated magnetic susceptibilities of Dy1 and Dy2 in complex **1DyGe** using CASSCF/RASSI with MOLCAS 8.2.

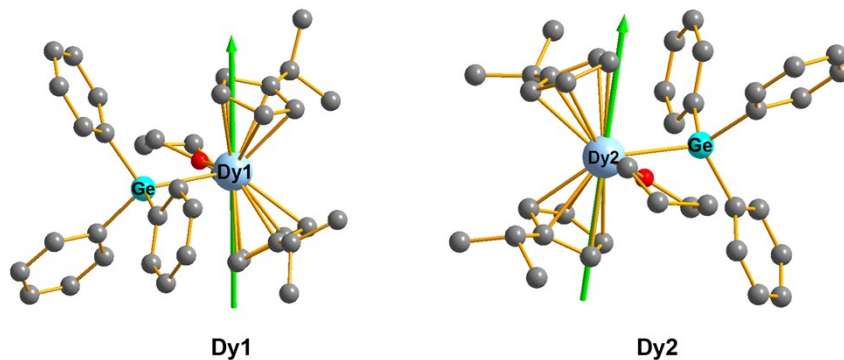


Figure S26. Calculated orientations of the local main magnetic axes on Dy1 and Dy2 in complex **1DyGe**.

4.2 *Ab initio* calculation for **1DySn**

Similar approach as **1DyGe**, and results are listed below.

Table S5. Calculated energy levels (cm^{-1}), g (g_x, g_y, g_z) tensors and m_J values of the lowest eight Kramers doublets (KDs) for **1DySn**.

1DySn			
KDs		E/cm^{-1}	g
			m_J
1	0.0	0.003 0.004 19.599	$\pm 15/2$
2	166.7	0.030 0.032 16.996	$\pm 13/2$
3	310.1	0.298 0.342 14.680	$\pm 11/2$
4	390.5	1.002 1.166 11.315	$\pm 5/2$
5	435.3	3.191 4.485 14.016	$\pm 9/2$
6	453.8	0.768 2.702 14.370	$\pm 3/2$
7	494.7	1.345 2.752 15.047	$\pm 7/2$
8	653.9	0.0104 0.0378 19.661	$\pm 1/2$

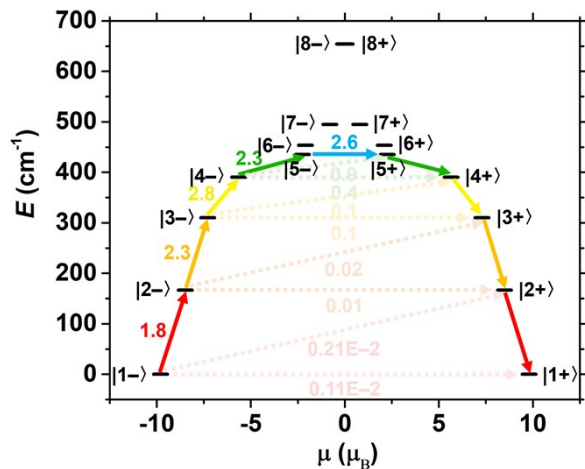


Figure S27. Magnetization blocking barriers for **1DySn**. The thick black lines represent the Kramers doublets as a function of their magnetic moment along the magnetic axis. The solid arrows represent the most probable path for magnetic relaxation in the corresponding compounds. The numbers at each arrow stand for the mean absolute value of the corresponding matrix element of transition magnetic moment.

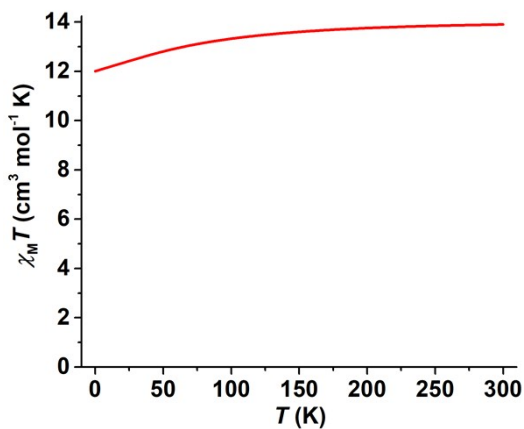


Figure S28. Calculated magnetic susceptibilities of **1DySn** using CASSCF/RASSI with MOLCAS 8.2.

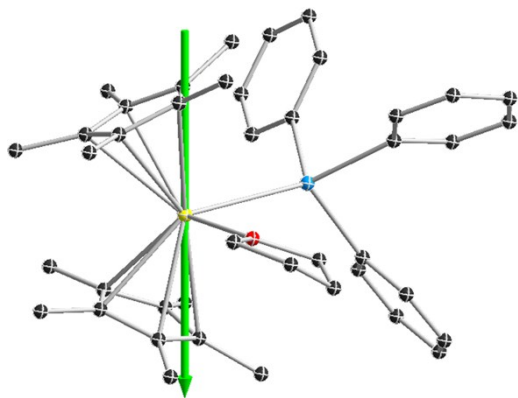


Figure S29. Calculated orientations of the local main magnetic axis in complex **1DySn**.

Table S6. Comparison of crystal field parameters of **1DyGe** (**Dy1/Dy2**) and **1DySn**.

$$H_{CF} = \sum_{\substack{k=2,4,6 \\ |q| \leq k}} (B_k^q \hat{O}_k^q)$$

<i>k</i>	<i>q</i>	<i>Bq k(1DyGe)</i>	<i>Bq k(1DySn)</i>
2	-2	0.79985036633478E+00/0.72154616221069E+00	-0.10776502452910E+01
2	-1	-0.77330232874771E-01/0.60451470755669E-01	-0.21553004905819E+01
2	0	-0.22310493074630E+01/-0.23813073780073E+01	-0.30993051847764E+01
2	1	0.10326274620717E+00/-0.13959720204604E+00	-0.40020116886481E+00
2	2	0.14876394166028E+01/0.22093817532791E+01	0.12035482025193E+01
4	-4	0.13230584154927E-01/0.14530553789335E-01	-0.13593865195777E-01
4	-3	-0.10335247601544E-01/-0.88072090159333E-02	-0.38449257049879E-01
4	-2	0.17763742340734E-02/0.71910438509598E-03	-0.10275996189761E-01
4	-1	0.26694462505762E-02/0.29092357575488E-02	-0.14532453178454E-01
4	0	-0.17033662237171E-02/-0.16375400646705E-02	-0.13062287887307E-02
4	1	-0.36440184409511E-02/-0.25244547811121E-02	-0.34408443944720E-03
4	2	0.33285212953344E-02/0.37719459511994E-02	0.33417656811155E-02
4	3	0.32715283174538E-02/-0.73087140999311E-03	-0.59517739803765E-02
4	4	-0.73723101849347E-02/-0.49436340120258E-02	-0.19233236137460E-02
6	-6	-0.15725512767786E-04/-0.29651077893340E-04	0.52754015141394E-04
6	-5	0.60800731401670E-04/0.77216386388502E-04	0.18274526905631E-03
6	-4	-0.12514906396463E-04/-0.22119272665651E-04	0.38961422273403E-04
6	-3	-0.31405246515270E-04/-0.68980242813814E-04	0.71133499505424E-04
6	-2	0.25881431957623E-03/0.23071775744877E-03	0.35566749752712E-04
6	-1	-0.12600858436289E-03/-0.17045327434253E-03	0.44988775275120E-04
6	0	0.66700527052717E-06/0.17825383272273E-05	-0.25763760189833E-06
6	1	0.72093329409139E-04/0.88020325313386E-04	0.35635257054318E-04
6	2	0.14134258860647E-03/0.19171226500548E-03	0.21815038887345E-03
6	3	0.16819658751962E-03/0.18676300154510E-03	0.30608850019959E-04
6	4	0.15161682801576E-04/0.21582901422476E-05	-0.36380991257909E-04
6	5	0.10402899336508E-03/0.79227389535785E-04	-0.30046598261745E-04
6	6	0.13837268104924E-04/-0.16752554723454E-04	-0.48979514264530E-04

4.3. Bonding Analyses

DFT calculations with UKS-BP86 functionals were carried out using Gaussian 09 Rev D.01 packages^[10] for bonding analysis. Second-order DKH treatment^[11] and ultrafine integral were

applied during the calculations. All electron Douglas-Kroll correlation consistent polarized basis sets were employed to describe metal ions: cc-pVTZ-DK3 for Dy^[12], cc-pVTZ-DK for Ge^[13] and Sn^[14]. 6-311G basis^[15] were used for C, H and O atoms. Molecular structures obtained from X-ray diffraction experiment were used without any further optimization since all measurement were performed on polycrystalline samples. NBO analysis was performed by NBO 3.1^[16] in G09 D package. Wavefunction analysis (Wiberg bond order, delocalization index) was performed using Multiwfn 3.6 program^[17], where near-grid method^[18] is employed to generate basins.

Table S7. Summary of Natural Bond Orbitals (NBO) of **1DyGe (Dy1/Dy2)** and **1DySn**

	NBO	Occupancy	Energy/Hartrees	Principal Delocalizations
Alpha Spin Orbitals	Dy(1)-Ge(2)	0.95165/0.95506	-0.34036/-0.34017	731(g),733(g),762(v),732(g) 768(v),764(v),191(g),201(g) 763(v),192(g),743(r),195(g) 204(g),730(g),767(v),734(r) 664(r),746(r),384(r),337(r) 336(r),735(r),448(r),772(r) 759(r),415(r),457(r),376(r) 392(r),367(r),563(r),755(r) 749(r)/
	Dy(1)-Sn(2)	0.95434	-0.38576	788(g),787(g),795(v),789(g) 797(v),792(v),191(g),202(g) 205(g),194(g),731(g),796(v) 791(v),741(r),312(r),732(r) 360(r),747(r),761(r),733(r) 400(r),315(r),408(r),744(r) 419(r),391(r),344(r),757(r) 437(r) 1020(g),1021(g),1022(g) 215(g),1019(g),229(g) 1051(v),1054(v),1057(v) 228(g),458(r),1026(r),432(r) 1037(r),1024(r),536(r) 1060(r),1069(r),1044(r) 1023(r),1032(r),1082(r) 393(r),484(r),537(r),460(r) 406(r),367(r),392(r),447(r) 407(r)
Beta Spin Orbitals	Dy(1)-Ge(2)	0.94666/0.94860	-0.31510/-0.32023	733(g),731(g),732(g),762(v) 185(g),764(v),768(v),184(g) 192(g),191(g),763(v),186(g) 196(g),767(v),743(r),448(r) 734(r),735(r),746(r),384(r) 664(r),338(r),759(r),772(r) 336(r),755(r),415(r),457(r) 337(r),467(r)/ 788(g),787(g),789(g),183(g) 795(v),797(v),191(g),792(v) 185(g),187(g),796(v),791(v) 186(g),192(g),741(r),732(r) 312(r),360(r),733(r),761(r) 315(r),747(r),400(r),744(r) 419(r),437(r),391(r),363(r) 757(r),408(r)

	Dy(1)-Sn(2)	0.95251	-0.38379	1022(g),1020(g),1021(g) 211(g),208(g),1019(g),220(g) 1051(v),210(g),209(g) 1054(v),1057(v),227(g) 458(r),1026(r),1037(r) 1024(r),536(r),432(r) 1060(r),1069(r),406(r) 1023(r),537(r),1082(r) 393(r),1032(r),447(r) 1044(r),382(r),433(r),484(r) 472(r)
--	-------------	---------	----------	--

Table S8. Summary of Natural Population Analysis of **1DyGe (Dy1/Dy2)** and **1DySn**

Compound	Atom	Natural Charge	Natural Population			
			Core	Valence	Rydberg	Total
1DyGe	Dy	1.32846/1.33828	53.98266/53.98370	10.47992/10.47716	0.20896/0.20086	64.67154/64.66172
	Ge	0.74959/0.72466	27.98564/27.98600	3.21447/3.23872	0.05030/0.05063	31.25041/31.27534
1DySn	Dy	1.35220	53.98101	10.39382	0.27297	64.64780
	Sn	0.92000	45.96899	3.06000	0.05102	49.08000

Table S9. Mulliken charges and spin densities with hydrogens summed into heavy atoms for **1DyGe (Dy1/Dy2)** and **1DySn**

Compound	Atom	Mulliken Charges	Spin Densities
1DyGe	Dy	1.387568/1.285633	4.932348/4.937958
	Ge	0.173093/0.253066	0.018018/0.003991
	O	-0.696012/-0.700681	0.000490/0.000579
1DySn	Dy	1.373802	4.917056
	Sn	0.745309	-0.018374
	O	-0.480663	0.000736

Table S10. Wiberg Bond order matrix for all electrons for **1DyGe (Dy1/Dy2)** (only part listed)

Atom No.	1(Dy)	2(Ge)	3(O)
1(Dy)	9.15613810/9.08194380	1.07865725/1.07026733	0.83745747/0.83342891
2(Ge)	1.07865725/1.07026733	5.13653536/5.09006192	0.00583810/0.00718543
3(O)	0.83745747/0.83342891	0.00583810/0.00718543	3.02306349/3.01173896

4(C)	0.47684920/0.49524872	0.00648821/0.00584121	0.00269463/0.00206968
5(C)	0.56254500/0.55799596	0.00530570/0.00530582	0.00092467/0.00094513
6(C)	0.57163655/0.51841195	0.00977086/0.00921406	0.00212410/0.00195412
7(C)	0.48312040/0.48910073	0.04066196/0.03235814	0.00132267/0.00195893
8(C)	0.50834585/0.53034872	0.00932179/0.00542881	0.00322296/0.00501018
9(C)	0.49429062/0.47749265	0.00679494/0.00443341	0.00136841/0.00135737
10(C)	0.52721917/0.53601995	0.005802000.00609994	0.00100840/0.00101679

Table S11. Wiberg Bond order matrix from mixed density for **1DyGe (Dy1/Dy2)** (only part listed)

Atom No.	1(Dy)	2(Ge)	3(O)
1(Dy)	8.98613096/8.91356086	1.04138415/1.04114864	0.83171378/0.82834861
2(Ge)	1.04138415/1.04114864	5.09763149/5.05903960	0.00582449/0.00714208
3(O)	0.83171378/0.82834861	0.00582449/0.00714208	3.01710408/3.00632489
4(C)	0.46827550/0.48606621	0.00638572/0.00578016	0.00268422/0.00206640
5(C)	0.55624028/0.54836434	0.00522770/0.00517205	0.00092016/0.00092860
6(C)	0.55614969/0.50813689	0.00941521/0.00915542	0.00209477/0.00191308
7(C)	0.47541586/0.47909846	0.04058983/0.03218595	0.00131698/0.00195738
8(C)	0.49869567/0.51401661	0.00928366/0.00507307	0.00317671/0.00491877
9(C)	0.48283664/0.46457715	0.00665514/0.00426424	0.00135342/0.00133014
10(C)	0.52078980/0.52603489	0.00574826/0.00600014	0.00098667/0.00100449

Table S12. Wiberg Bond index matrix in the natural atomic orbitals (NAO) basis for **1DyGe (Dy1/Dy2)** (only part listed)

Atom No.	1(Dy)	2(Ge)	3(O)
1(Dy)	0.0000/0.0000	0.6689/0.6685	0.1838/0.1875
2(Ge)	0.6689/0.6685	0.0000/0.0000	0.0019/0.0024
3(O)	0.1838/0.1875	0.0019/0.0024	0.0000/0.0000
4(C)	0.1252/0.1246	0.0027/0.0033	0.0013/0.0009
5(C)	0.1619/0.1567	0.0026/0.0022	0.0007/0.0005
6(C)	0.1587/0.1449	0.0033/0.0037	0.0013/0.0012

7(C)	0.1329/0.1408	0.0180/0.0152	0.0009/0.0015
8(C)	0.1457/0.1577	0.0048/0.0025	0.0011/0.0016
9(C)	0.1354/0.1351	0.0027/0.0027	0.0013/0.0014
10(C)	0.1566/0.1594	0.0025/0.0035	0.0008/0.0009

Table S13. Atom-atom overlap-weighted NAO bond order for **1DyGe (Dy1/Dy2)** (only part listed)

Atom No.	1(Dy)	2(Ge)	3(O)
1(Dy)	0.0000/0.0000	0.7314/0.7385	0.1928/0.1978
2(Ge)	0.7314/0.7385	0.0000/0.0000	0.0045/0.0045
3(O)	0.1928/0.1978	0.0045/0.0045	0.0000/0.0000
4(C)	0.2134/0.2056	0.0009/0.0028	0.0032/0.0011
5(C)	0.2548/0.2330	0.0028/0.0007	-0.0001/0.0001
6(C)	0.2510/0.2400	0.0028/0.0023	0.0003/0.0002
7(C)	0.2263/0.2403	0.0444/0.0371	-0.0002/-0.0003
8(C)	0.2365/0.2484	-0.0029/-0.0004	0.0027/0.0049
9(C)	0.2141/0.2126	0.0011/0.0000	0.0002/0.0002
10(C)	0.2449/0.2404	0.0025/0.0033	-0.0001/-0.0002

Table S14. Orbital contributions to the bond Dy–Ge in **1DyGe (Dy1/Dy2)**

	Contribution/%					
	Atom	Orbitals				
Alpha Spin Orbitals	Dy	<i>s</i>	<i>p</i> 0.74/0.81	<i>d</i> 1.57/1.48	<i>f</i> 0.01	<i>g</i> 0.00
	22.08/21.93	30.09/30.29	22.33/24.61	47.33/ 44.90	0.25/ 0.20	0.01/ 0.01
	Ge	<i>s</i>	<i>p</i> 1.57/1.56	<i>d</i> 0.01	<i>f</i> 0.00	
	77.92/78.07	38.79/38.92	60.96/ 60.84	0.25/ 0.24	0.00/0.00	
Beta Spin Orbitals	Dy	<i>s</i>	<i>p</i> 0.82/0.90	<i>d</i> 1.47/1.46	<i>f</i> 1.19/0.92	<i>g</i> 0.00
	27.46/25.84	22.36/23.34	18.24/21.04	32.81/34.19	26.60/21.42	0.00/0.00
	Ge	<i>s</i>	<i>p</i> 1.94/1.85	<i>d</i> 0.01	<i>f</i> 0.00	

	72.54/74.16	33.91/35.04	65.89/64.76	0.20/0.20	0.00/0.00
--	-------------	-------------	-------------	-----------	-----------

Table S15. Wiberg Bond order matrix for all electrons for **1DySn** (only part listed)

Atom No.	1(Dy)	2(Sn)	3(O)	4(C)	5(C)
1(Dy)	8.92896540	1.03704996	0.81087334	0.50050686	0.48444315
2(Sn)	1.03704996	5.00294404	0.00720527	0.00756145	0.02752020
3(O)	0.81087334	0.00720527	3.22278578	0.00113849	0.00114858
4(C)	0.50050686	0.00756145	0.00113849	4.49884702	1.18673172
5(C)	0.48444315	0.02752020	0.00114858	1.18673172	4.50741144
6(C)	0.47663360	0.00542640	0.00494900	0.11771325	1.19963461
7(C)	0.49189017	0.00448879	0.00097410	1.19780477	0.11779852
8(C)	0.49997299	0.00397243	0.00179785	0.00211103	0.00061525
9(C)	0.49171623	0.00430773	0.00200399	0.12140060	0.11900573
10(C)	0.47887441	0.01740808	0.00096356	0.00043600	0.00070075

Table S16. Wiberg Bond order matrix from mixed density for **1DySn** (only part listed)

Atom No.	1(Dy)	2(Sn)	3(O)	4(C)	5(C)
1(Dy)	8.73168590	1.02291252	0.80514379	0.48851292	0.46937055
2(Sn)	1.02291252	4.98801734	0.00719686	0.00755121	0.02745347
3(O)	0.80514379	0.00719686	3.21668722	0.00113000	0.00112761
4(C)	0.48851292	0.00755121	0.00113000	4.48634986	1.18672577
5(C)	0.46937055	0.02745347	0.00112761	1.18672577	4.49139693
6(C)	0.45881452	0.00528098	0.00488693	0.11768320	1.19953610
7(C)	0.47721274	0.00439300	0.00092211	1.19779393	0.11772390
8(C)	0.48482346	0.00388328	0.00175385	0.00202778	0.00046528
9(C)	0.47908903	0.00427750	0.00199697	0.12134213	0.11895177
10(C)	0.46667170	0.01737561	0.00094942	0.00039523	0.00068524

Table S17. Wiberg Bond index matrix in the NAO basis for **1DySn** (only part listed)

Atom No.	1(Dy)	2(Sn)	3(O)	4(C)	5(C)	6(C)	7(C)	8(C)	9(C)
1(Dy)	0.0000	0.7047	0.1462	0.1235	0.1248	0.1223	0.1301	0.1232	0.1260
2(Sn)	0.7047	0.0000	0.0025	0.0025	0.0134	0.0033	0.0024	0.0035	0.0028
3(O)	0.1462	0.0025	0.0000	0.0011	0.0011	0.0026	0.0007	0.0013	0.0012
4(C)	0.1235	0.0025	0.0011	0.0000	1.2949	0.0517	1.3056	0.0021	0.0614
5(C)	0.1248	0.0134	0.0011	1.2949	0.0000	1.3002	0.0538	0.0005	0.0558
6(C)	0.1223	0.0033	0.0026	0.0517	1.3002	0.0000	0.0575	0.0010	1.3027
7(C)	0.1301	0.0024	0.0007	1.3056	0.0538	0.0575	0.0000	0.0041	1.2889
8(C)	0.1232	0.0035	0.0013	0.0021	0.0005	0.0010	0.0041	0.0000	0.0025
9(C)	0.1260	0.0028	0.0012	0.0614	0.0558	1.3027	1.2889	0.0025	0.0000
10(C)	0.1183	0.0064	0.0004	0.0009	0.0013	0.0039	0.0012	1.3077	0.0014

Table S18. Atom-atom overlap-weighted NAO bond order for **1DySn** (only part listed)

Atom No.	1(Dy)	2(Sn)	3(O)	4(C)	5(C)	6(C)	7(C)	8(C)	9(C)
1(Dy)	0.0000	0.8352	0.1586	0.2125	0.2196	0.2046	0.2116	0.2091	0.2217
2(Sn)	0.8352	0.0000	0.0038	0.0002	0.0302	-0.0014	0.0021	-0.0007	0.0030
3(O)	0.1586	0.0038	0.0000	0.0002	-0.0005	0.0070	0.0000	0.0003	0.0004
4(C)	0.2125	0.0002	0.0002	0.0000	1.1107	-0.0176	1.1141	0.0045	-0.0220
5(C)	0.2196	0.0302	-0.0005	1.1107	0.0000	1.1132	-0.0185	-0.0003	-0.0176
6(C)	0.2046	-0.0014	0.0070	-0.0176	1.1132	0.0000	-0.0189	0.0003	1.1125
7(C)	0.2116	0.0021	0.0000	1.1141	-0.0185	-0.0189	0.0000	0.0096	1.1092
8(C)	0.2091	-0.0007	0.0003	0.0045	-0.0003	0.0003	0.0096	0.0000	-0.0015
9(C)	0.2217	0.0030	0.0004	-0.0220	-0.0176	1.1125	1.1092	-0.0015	0.0000
10(C)	0.2127	0.0182	0.0000	-0.0005	-0.0004	0.0006	-0.0008	1.1154	0.0005

Table S19. Orbital contributions to the bond Dy–Sn in **1DySn**

		Contribution/%				
		Atom	Orbitals			
Alpha Spin Orbitals		Dy	s	p 0.85	d 1.37	f 0.01
		22.76	31.49	26.90	41.27	0.33
						0.01

	Sn	s	p 1.29	d 0.01	f 0.00
	77.24	43.52	56.14	0.34	0.00
Beta Spin Orbitals	Dy	s	p 0.95	d 1.29	f 0.46
	24.95	27.01	25.66	34.85	12.48
	Sn	s	p 1.35	d 0.01	f 0.00
	75.05	42.40	57.32	0.27	0.00

Table S20. Total delocalization index matrix for **1DyGe (Dy1/Dy2)** (only part listed)

Atom	Dy	Ge	O
Dy	3.46778064/2.98725528	0.46220442/0.45144514	0.27917072/0.27608260
Ge	0.46220442/0.45144514	2.99953804/3.43573038	0.01298296/0.01506536
O	0.27917072/0.27608260	0.01298296/0.01506536	2.55122205/2.54627699
C1	0.18196553/0.20784944	0.00736268/0.00520832	0.01350545/0.00504654
C2	0.21513142/0.19988280	0.00731376/0.00808977	0.00249492/0.00247925
C3	0.21785070/0.20473222	0.01218429/0.00606405	0.00571306/0.01625896
C4	0.17791826/0.18456516	0.05174384/0.01812040	0.00222884/0.01687685
C5	0.18591809/0.18825040	0.01251287/0.03937465	0.01746111/0.00254174

Table S21. Total delocalization index matrix for **1DySn** (only part listed)

Atom	Dy	Sn	O	C1	C2	C3
Dy	3.02637619	0.38297073	0.27407090	0.20606903	0.20947147	0.20518570
Sn	0.38297073	3.36214426	0.01616613	0.00592220	0.01082154	0.04464882
O	0.27407090	0.01616613	2.55557805	0.00276027	0.00454024	0.00310283
C1	0.20606903	0.00592220	0.00276027	4.31540488	1.27181753	0.09684740
C2	0.20947147	0.01082154	0.00454024	1.27181753	4.31279257	1.26037178
C3	0.20518570	0.04464882	0.00310283	0.09684740	1.26037178	4.32652948
C4	0.19426223	0.00647348	0.02466497	0.09759895	0.09807068	1.26806492
C5	0.20641431	0.00668261	0.00912849	1.25981784	0.10178614	0.09742014

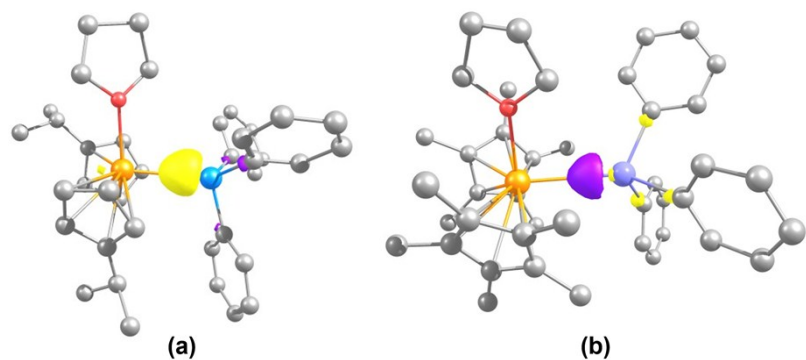


Figure S30. Ln–M (M = Ge, Sn) bonding interaction in the HOMO–1 of **1DyGe** (a) and **1DySn** (b) of the α -spin orbitals at the $0.05 \text{ e } \text{\AA}^{-3}$ contour surface.

References

- [1] W. J. Evans, M. A. Johnston, M. A. Greci, T. S. Gummersheimer and J. W. Ziller, *Polyhedron*, **2003**, *22*, 119.
- [2] R. J. P. Corriu and C. Guerin, *J. Organomet. Chem.*, **1980**, *197*, C19.
- [3] S. Demir, J. M. Zadrozny, M. Nippe and J. R. Long, *J. Am. Chem. Soc.*, **2012**, *134*, 18546.
- [4] W. J. Evans, B. L. Davis, T. M. Champagne and J. W. Ziller, *Proc. Natl. Acad. Sci. U.S.A.*, **2006**, *103*, 12678.
- [5] O. V. Dolomanov, L. J. Bourhis, R. J. Gildea, J. A. K. Howard and H. Puschmann, *J. Appl. Cryst.*, **2009**, *42*, 339.
- [6] L. Palatinus and G. Chapuis, *J. Appl. Cryst.*, **2007**, *40*, 786.
- [7] G. A. Bain and J. F. Berry, *J. Chem. Edu.*, **2008**, *85*, 532.
- [8] G. Karlström, R. Lindh, P. Å. Malmqvist, B. O. Roos, U. Ryde, V. Veryazov, P. O. Widmark, M. Cossi, B. Schimmelpfennig, P. Neogrady and L. Seijo, *Comput. Mater. Sci.*, **2003**, *28*, 222.
- [9] (a) L. F. Chibotaru, L. Ungur and A. Soncini, *Angew. Chem. Int. Ed.*, **2008**, *47*, 4126. (b) L. Ungur, W. Van den Heuvel and L. F. Chibotaru, *New J. Chem.*, **2009**, *33*, 1224. (c) L. F. Chibotaru, L. Ungur, C. Aronica, H. Elmoll, G. Pilet and D. Luneau, *J. Am. Chem. Soc.*, **2008**, *130*, 12445.
- [10] M. J. Frisch, G. W. Trucks, H. B. Schlegel, G. E. Scuseria, M. A. Robb, J. R. Cheeseman, G. Scalmani, V. Barone, B. Mennucci, G. A. Petersson, H. Nakatsuji, M. Caricato, X. Li, H. P. Hratchian, A. F. Izmaylov, J. Bloino, G. Zheng, J. L. Sonnenberg, M. Hada, M. Ehara, K. Toyota, R. Fukuda, J. Hasegawa, M. Ishida, T. Nakajima, Y. Honda, O. Kitao, H. Nakai, T. Vreven, J. A. Montgomery, Jr., J. E. Peralta, F. Ogliaro, M. Bearpark, J. J. Heyd, E. Brothers, K. N. Kudin, V. N. Staroverov, T. Keith, R. Kobayashi, J. Normand, K. Raghavachari, A. Rendell, J. C. Burant, S. S. Iyengar, J. Tomasi, M. Cossi, N. Rega, J. M. Millam, M. Klene, J. E. Knox, J. B. Cross, V. Bakken, C. Adamo, J. Jaramillo, R. Gomperts, R. E. Stratmann, O. Yazyev, A. J. Austin, R. Cammi, C. Pomelli, J. W. Ochterski, R. L. Martin, K. Morokuma, V. G. Zakrzewski, G. A. Voth, P. Salvador, J. J. Dannenberg, S. Dapprich, A. D. Daniels, O. Farkas, J. B. Foresman, J. V. Ortiz, J. Cioslowski and D. J. Fox, Revision D.01 ed., Gaussian, Inc., Wallingford CT, **2013**.
- [11] (a) B. A. Hess, *Phys. Rev. A*, **1985**, *32*, 756. (b) B. A. Hess, *Phys. Rev. A*, **1986**, *33*, 3742. (c) G. Jansen and B. A. Hess, *Phys. Rev. A*, **1989**, *39*, 6016. (d) M. Douglas and N. M. Kroll, *Annals of Physics*, **1974**, *82*, 89.
- [12] Q. Lu and K. A. Peterson, *J. Chem. Phys.*, **2016**, *145*, 054111.
- [13] A. K. Wilson, D. E. Woon, K. A. Peterson and T. H. Dunning, *J. Chem. Phys.*, **1999**, *110*, 7667.
- [14] D. H. Bross and K. A. Peterson, *Theo. Chem. Acc.*, **2013**, *133*, 1434.
- [15] G. A. Petersson, A. Bennett, T. G. Tensfeldt, M. A. Al-Laham, W. A. Shirley and J. Mantzaris, *J. Chem. Phys.*, **1988**, *89*, 2193.
- [16] (a) E. D. Glendening, A. E. Reed, J. E. Carpenter and F. Weinhold, 3.1 Ed. (b) J. P. Foster and F. Weinhold, *J. Am. Chem. Soc.*, **1980**, *102*, 7211. (c) A. E. Reed and F. Weinhold, *J. Chem. Phys.*, **1983**, *78*, 4066. (d) A. E. Reed, R. B. Weinstock and F. Weinhold, *J. Chem. Phys.*, **1985**, *83*, 735. (e) A. E. Reed and F. Weinhold, *J. Chem. Phys.*, **1985**, *83*, 1736. (f) J. E. Carpenter and F. Weinhold, *J. Mol. Struct.: Theochem.*, **1988**, *169*, 41. (g) A. E. Reed, L. A. Curtiss and F. Weinhold, *Chem. Rev.*, **1988**, *88*, 899.
- [17] (a) T. Lu and F. Chen, *J. Comput. Chem.*, **2012**, *33*, 580. (b) T. Lu and F. Chen, *Acta Chim. Sinica*, **2011**, *69*, 2393.
- [18] W. Tang, E. Sanville and G. Henkelman, *J. Phys. Condens. Matter* **2009**, *21*, 084204.